Photonic generation of arbitrary waveforms based on incoherent wavelength-to-time mapping*

Dong Jian-Ji(董建绩)†, Luo Bo-Wen(罗博文),
Yu Yuan(于 源), and Zhang Xin-Liang(张新亮)

Wuhan National Laboratory for Optoelectronics, School of Optoelectronic Science and Engineering, Huazhong University of Science and Technology, Wuhan 430074, *China*

(Received 29 August 2011; revised manuscript received 29 November 2011)

We demonstrate experimentally a radio frequency arbitrary waveform generator using the incoherent wavelength-to-time mapping technique. The system is implemented by amplitude modulation of a broadband optical resource whose spectrum is reshaped by a programmable optical pulse shaper and transmitted over a single mode fiber link. The shape of the generated waveform is controlled by the optical pulse shaper, and the fiber link introduces a certain group velocity delay to implement wavelength-to-time mapping. Assisted by the flexible optical pulse shaper, we obtain different shapes of optical waveforms, such as rectangle, triangle, and sawtooth waveforms. Furthermore, we also demonstrate ultra-wideband generation, such as Gaussian monocycle, doublet, and triplet waveforms, using the incoherent technique.

Keywords: arbitrary waveform generation, ultra-wideband, wavelength-to-time mapping, incoherent technique

PACS: 84.40.–x, 42.79.Sz, 47.27.De **DOI:** 10.1088/1674-1056/21/6/068401

1. Introduction

High frequency and large bandwidth arbitrary waveform generation has become an important research area that has numerous scientific and industrial applications, such as ultra-wideband (UWB) communications, pulsed radar systems and sensor networks. Due to the limited sampling rate, the generation of an arbitrary waveform in the electrical domain is limited to a low frequency and small bandwidth. A feasible solution is optical arbitrary waveform generation (OAWG), which can take advantage of the high speed and broad bandwidth offered by modern optics. OAWG reveals lots of potential applications where the manipulation of amplitude and phase of the optical signal with a tremendous bandwidth are required. Such applications include high-frequency microwave signal processing,[1−4] UWB-over-fiber communications,[5] high speed optical communications,[6,7] and dispersion compensation in optical fiber communications.[8]

Generally, OAWG can be classified into four categories, i.e., space-to-time pulse shaping,[9,10] temporal pulse shaping,[11] photonic microwave delay line filtering,[12] wavelength-to-time mapping,[3,4,13] and so on. Each category has its own advantages. Especially, the wavelength-to-time mapping technique is very flexible and robust since the spectral shape is easily changed in the frequency domain, including both coherent techniques and incoherent techniques. Coherent techniques offer high-fidelity output waveforms with expensive coherent sources.[14,15] For example, Wang *et al.*[14] proposed an OAWG using wavelength-to-time mapping via a chirped fiber Bragg grating. The incoherent wavelength-to-time mapping concept was proposed and demonstrated first by Dorrer,[16] offering a low-cost solution but the output waveform had a low signal-to-noise ratio. Company *et al.*[17] demonstrated an incoherent technique to generate arbitrary radio frequency (RF) waveform using a commercial dense wavelength division multiplexing (DWDM) controller. However the frequency channel span was over 100 GHz with a coarse resolution. Similar methods were also presented in Refs. [13] and [18]. However, once the frequency device was fabricated its spectral shape could not be freely reconfigured. Hence the OAWG was not flexible.

In this paper, we propose and demonstrate a simple OAWG scheme using the incoherent wavelength-

*Project supported by the National Basic Research Program of China (Grant No. 2011CB301704), the National Natural Science Foundation of China (Grant Nos. 60901006 and 11174096), and the Fundamental Research Funds for the Central Universities of China (Grant No. 2010QN033).

†Corresponding author. E-mail: jjdong@mail.hust.edu.cn

© 2012 Chinese Physical Society and IOP Publishing Ltd

to-time mapping technique. The system is implemented by intensity modulation of a broadband amplified spontaneous emission (ASE) source, whose spectrum is reshaped by a programmable optical pulse shaper and transmitted over a single mode fiber (SMF) link. The shape of the generated waveform is controlled by the optical pulse shaper with a high resolution of 10 GHz, and the SMF introduces a group velocity dispersion (GVD) to achieve wavelength-to-time mapping. Assisted by the flexible optical pulse shaper, we obtain different optical waveforms, such as rectangle, triangle, and sawtooth waveforms. Furthermore, UWB pulse signals, such as Gaussian monocycle, doublet, and triplet waveforms are also demonstrated using the incoherent technique. Due to the flexible optical pulse shaper, the generated waveforms can be freely reconfigured.

2. Experimental setup and operation principle

The experimental setup of the OAWG scheme is shown in Fig. 1. The system consists of a broadband ASE source, an optical pulse shaper, a Mach–Zehnder modulator (MZM), and an SMF link. The broadband source is offered by two cascaded erbium-doped fiber amplifiers (EDFAs), whose output spectrum is shown in the inset of Fig. 1. The broadband source is intensity-modulated by the MZM, which is driven by the bit pattern generator (BPG). A programmable optical pulse shaper (Finisar Company) is employed to design user-specified spectral shapes, such as rectangular or triangular shapes. The optical pulse shaper is based on spatial diffraction and liquid crystal on silicon switching elements, and both spectral amplitude and phase are programmable. Hence, arbitrary spectral shape can be designed within a C-band. The minimum programmable filter bandwidth is 10 GHz. The detailed operation principle of the optical pulse shaper has been discussed in Refs. [19] and [20]. Consequently, an SMF link then introduces a GVD to achieve wavelength-to-time mapping. Then the user-specified spectral shape is mapped into the designed temporal waveform accordingly. Finally, the temporal waveforms, and optical spectra are analysed through a digital communication analyser (Agilent DCA86100C), and an optical spectral analyser (OSA, Anritsu MS9710C), respectively.

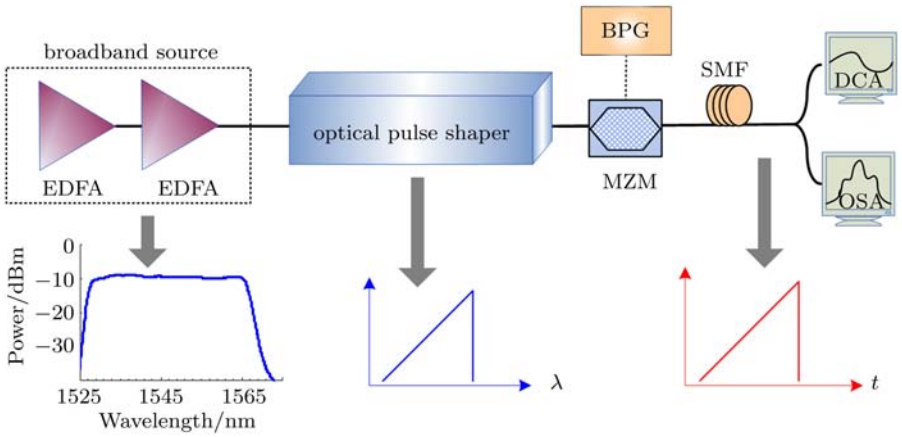


Fig. 1. (colour online) Experimental setup of the proposed scheme.

The incoherent wavelength-to-time mapping process can be mathematically explained. Assume that the optical pulse shaper has a user-specified spectral density function $I(\lambda)$ and the generated optical pulse driven by the BPG is expressed by $s(t)$. The broadband ASE source is approximately a constant in the EDFA gain spectrum range. Due to the GVD of the SMF, the output temporal waveform can be described as

$$g(t) = \int I(\lambda) \cdot s[t - T(\lambda)] \mathrm{d}\lambda, \tag{1}$$

where $T(\lambda)$ is the relevant time delay induced by the GVD of the SMF, written as $T(\lambda) = DL(\lambda - \lambda_0)$, where D, L, λ, and λ_0 denote the SMF dispersion parameter, the fiber length, the optical wavelength, and zero-dispersion wavelength, respectively.

In our experiment, the modulated optical pulse shows very small pulsewidth compared with the pulse period. Therefore, $s(t)$ can be approximately regarded as a unit impulse function $\delta(t)$. Then equation (1) can be replaced by

$$g(t) = \int I(\lambda) \cdot \delta[t - DL(\lambda - \lambda_0)]\,\mathrm{d}\lambda = I(t/DL + \lambda_0). \quad (2)$$

Equation (2) indicates that the designed spectral shape is mapped into the temporal waveform accordingly.

3. Experimental results and discussion

In the experiment, an optical Gaussian pulse sequence with a repetition rate of 1.25 GHz is generated by the BPG without transmission in the SMF as shown in Fig. 2. The optical pulse shaper is not inserted in the system. The pulse period is 800 ps. For single pulse duration, the rise time and the fall time are about 28 ps and 35 ps, respectively. The pulsewidth is about 36 ps, which determines the time resolution of arbitrary waveform generation. It should be noted that incoherent wavelength-to-time mapping for OAWG has a main drawback of low signal-to-noise ratio. Therefore the measured waveforms from the DCA are normally the average of the intensity. The temporal waveforms are obtained by averaging 8 time measurements.

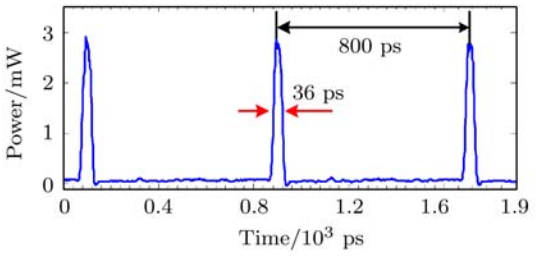


Fig. 2. (colour online) Gaussian pulse sequence generated by the BPG.

Then the optical pulse shaper is inserted into the system, and the modulated signal is transmitted in the SMF. The SMF dispersion parameter D is 17.6 ps/km/nm, and the SMF length is initially fixed at 1 km. When the optical pulse shapers are designed with a spectral density function of rectangle, sawtooth, and triangle respectively, the output spectra are shown in Figs. 3(a), 3(b) and 3(c). The programmed spectrum span is 12.8 nm centred at 1550 nm. The solid lines and the dashed lines represent measured spectra from the OSA and the designed spectra, respectively. One can see that the measured and the designed spectral shapes are consistent with each other. The generated temporal waveforms are shown in Figs. 4(a), 4(b), and 4(c), respectively. There is a little fluctuation

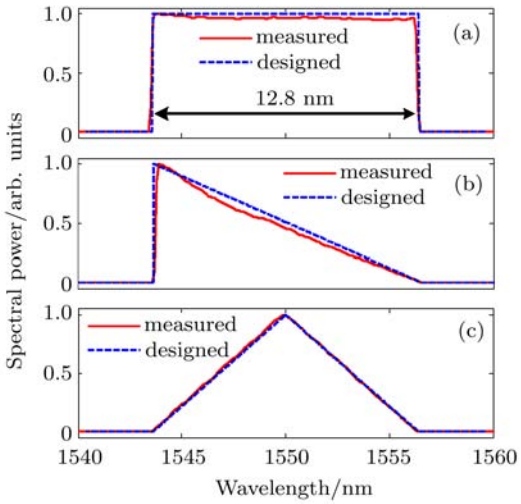


Fig. 3. (colour online) Output spectra of the designed optical pulse shaper, showing rectangle (a), sawtooth (b), and triangle (c) waveforms. The solid lines and the dashed lines represent measured and designed spectra, respectively.

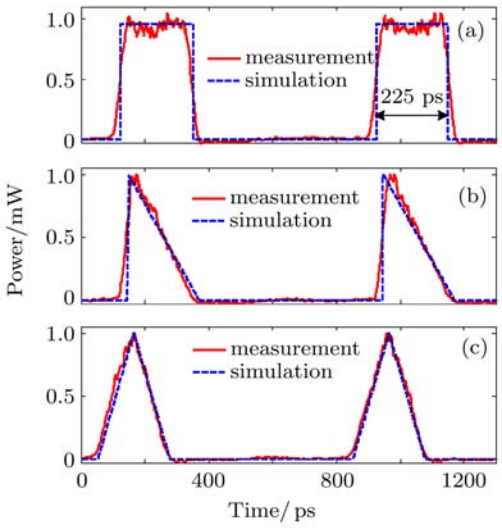


Fig. 4. (colour online) Generated temporal waveforms obtained by averaging 8 time measurements, showing rectangle (a), sawtooth (b), and triangle (c) waveforms. The solid lines and the dashed lines represent measured and simulated waveforms, respectively.

on the top of each waveform. This is caused mainly by the ASE broadband source. The simulation results are also plotted as dashed lines for comparison. From the

measured waveforms, we can observe that the pulse duration is about 225 ps. In theory, the pulse duration is calculated by $\Delta T = DL\Delta\lambda$, where $\Delta\lambda$ is the programmed spectrum span. Then the pulse duration is calculated to be 225.3 ps. So the measured pulse duration is in accordance with the calculated one.

Since the pulse duration is determined by $\Delta T = DL\Delta\lambda$, we can optimize the SMF length and the spectrum span to ensure that the pulse duration can fill the whole temporal period. Furthermore, UWB pulses can be obtained if the spectral shape is designed as the shape of the Gaussian derivatives. For example, the 1-km SMF is replaced by another 2-km SMF, and the programmed spectrum span is set at 23 nm so that the pulse duration is around 800 ps, equal to the temporal period. When the optical pulse shapers are designed, respectively, with a spectral density function of Gaussian monocycle, doublet, and triplet waveforms, the output spectra are shown as curves S_1, S_2, and S_3 in Fig. 5. The solid lines and the dashed lines represent the measured spectra and the designed spectra, respectively. Again, the measured spectra accords well with the designed spectra. The generated temporal UWB waveforms are shown correspondingly as curves W_1, W_2, and W_3 in Fig. 5. The designed waveforms are also plotted as dashed lines for comparison. Similarly, the generated UWB waveforms accord well with the simulated temporal waveforms except a little amplitude fluctuation on the top. The pulsewidths of all generated UWB pulses are larger than 90 ps. In fact, the pulsewidth can be adjusted by designing the optical pulse shaper.

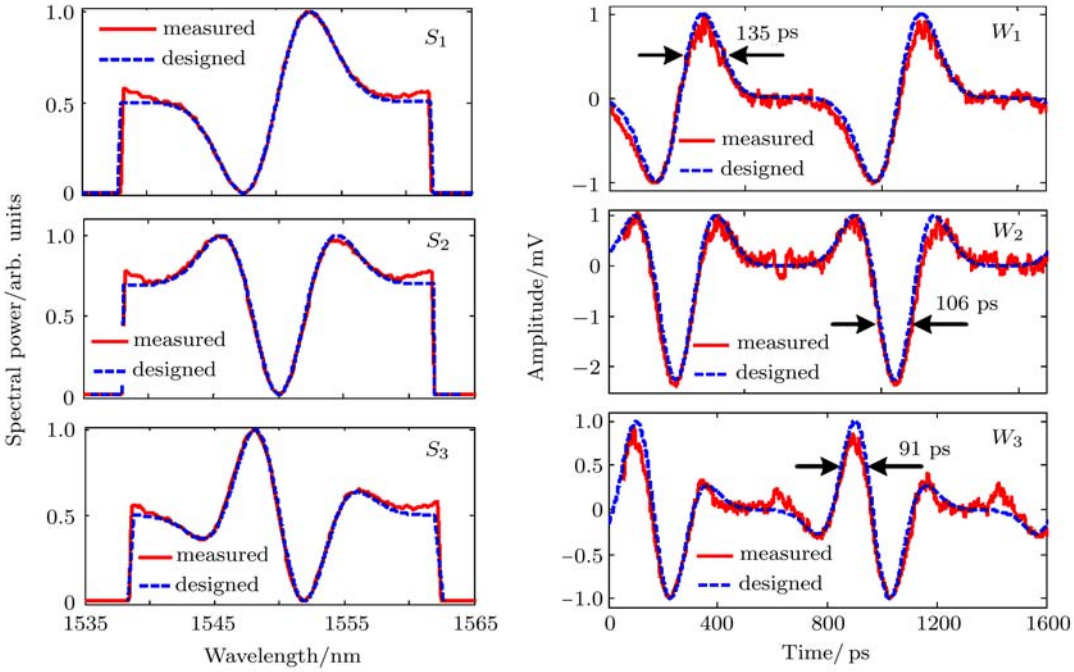


Fig. 5. (colour online) Output spectra (S_1, S_2, S_3) and temporal waveforms (W_1, W_2, W_3) obtained by averaging 8 time measurements, showing designed Gaussian monocycle (a), doublet (b), and triplet (c) waveforms. The solid lines and the dashed lines represent measured and simulated results, respectively.

Figure 6 shows the RF spectra of generated UWB waveforms: (a) monocycle waveform, (b) doublet waveform, (c) and triplet waveform, respectively. The dashed lines represent the RF spectral envelopes of standard monocycle, doublet, and triplet waveforms, respectively. The central frequencies (CFs) are 1.9 GHz, 2.7 GHz, and 3.2 GHz for the monocycle, the doublet, and the triplet waveforms, respectively. And the corresponding 10-dB bandwidths (BWs) are 3.8 GHz, 4 GHz, and 4.1 GHz respectively.

It should be noted that the CF and 10-dB BW of the RF spectra can be increased as the pulsewidth of UWB waveform is decreased. In order to increase the 10-dB BW of the RF spectrum, we may design a narrower spectral UWB shape $I(\lambda)$, in the meantime we use the programmed spectrum span $\Delta\lambda$. At the same time, carrier suppression effect (CSE) is inevitable due to SMF dispersion in microwave signal processing. However, the SMF length is only 1-km or 2-km long, so the first notch of the CSE is larger than 40 GHz, which is beyond the frequency band of our interest. Hence the CSE can be ignored in our scheme.

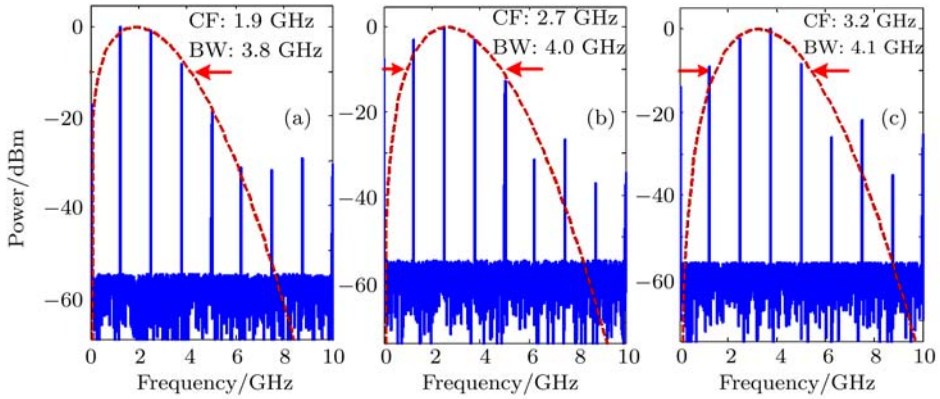


Fig. 6. (colour online) RF spectra of generated (a) monocycle, (b) doublet, and (c) triplet waveforms. The dashed lines represent the RF spectral envelopes of standard monocycle (a), doublet (b), and triplet (c) waveforms, respectively.

4. Conclusions

We proposed and demonstrated an OAWG scheme using the incoherent wavelength-to-time mapping technique. The configuration consists of a broadband ASE source modulated by an MZM, a programmable optical pulse shaper to reshape a user-specified spectrum, and an SMF link to implement wavelength-to-time mapping. Assisted by the flexible optical pulse shaper, we obtained different shapes of optical waveforms, such as rectangle, triangle, and sawtooth waveforms. We also demonstrated the applications of our scheme in UWB RF signal generation, such as Gaussian monocycle, doublet, and triplet waveforms. Due to the flexible optical pulse shaper, the generated waveforms can be freely changed.

References

[1] Yao J P 2011 *Opt. Commun.* **284** 3723
[2] Zou H, Zhu W H and Wang G D 2007 *Chin. Phys.* **16** 3429
[3] Yao J P 2010 *Nature Photon.* **4** 79
[4] Dong J J, Zhang X L, Yu Y, Xu J and Huang D X 2008 *Chin. Phys. Lett.* **25** 911
[5] Dong J J, Zhang X L and Huang D X 2008 *Chin. Phys.* B **17** 4226
[6] Dong J J, Zhang X L, Wang Y and Huang D X 2008 *Acta Phys. Sin.* **57** 2222 (in Chinese)
[7] Dong J J, Zhang X L, Fu S N, Xu J, Shum P and Huang D X 2008 *Journal of Selected Topics in Quantum Electronics* **14** 770
[8] Cartledge J C, Jiang Y, Karar A S, Harley J and Roberts K 2011 *Opt. Commun.* **284** 3711
[9] Jiang Z, Huang C B, Leaird D E and Weiner A M 2007 *Nature Photon* **1** 463
[10] Kuo F M, Shi J W, Chiang H C, Chuang H P, Chiou H K, Pan C L, Chen N W, Tsai H J and Huang C B 2010 *Photon. J. IEEE* **2** 719
[11] Azaña J, Berger N K, Levit B and Fischer B 2006 *J. Lightwave Technol.* **24** 2663
[12] Mingya S and Minasian R A 2004 *Photon. Technol. Lett. IEEE* **16** 1155
[13] Bolea M, Mora J, Ortega B and Capmany J 2011 *IEEE Photo. Technol. Lett.* **23** 618
[14] Wang C and Yao J P 2008 *Proc. Microsystems and Nanoelectronics Research Conference* October 14–15, 2008, Ottawa, Canada p. 57
[15] Lin I S, McKinney J D and Weiner A M 2005 *Microwave and Wireless Components Letters* **15** 226
[16] Dorrer C 2004 *J. Opt. Soc. Am.* B **21** 1417
[17] Torres-Company V, Lancis J, Andrés P and Chen L R 2008 *J. Lightwave Technol.* **26** 2476
[18] Wang C and Yao J P 2009 *Broadband Network & Multimedia Technology, 2009, IC-BNMT '09* 909
[19] Dong J J, Yu Y, Zhang Y, Luo B W, Yang T and Zhang X L 2011 *Photon. J.* **3** 996
[20] Dong J J, Luo B W, Zhang Y, Lei L, Huang D X and Zhang X L 2012 *Chin. Phys. Lett.* **29** 014203